C2012-0001322

NACE INTERNATIONAL CORROSION 2012 CONFERENCE & EXPO

Effects of CO_2 Phase Change, SO_2 Content and Flow on the Corrosion of CO_2 Transmission Pipeline Steel

F. Farelas
Institute for Corrosion and Multiphase Technology, Department of Chemical & Biomolecular Engineering, Ohio University, Athens, OH 45701, USA

Y.S. Choi
Institute for Corrosion and Multiphase Technology, Department of Chemical & Biomolecular Engineering, Ohio University, Athens, OH 45701, USA

S. Nesic
Institute for Corrosion and Multiphase Technology, Department of Chemical & Biomolecular Engineering, Ohio University, Athens, OH 45701, USA

ABSTRACT

Results from previous studies demonstrated that significant corrosion of carbon steel was observed when 1% SO_2 impurity was contained in a supercritical CO_2 phase in the presence of small amounts of water (650 ppm). Considering real situations for CO_2 transportation pipelines, the effects of CO_2 phase change, impurity concentration and flow were evaluated in the present study in order to establish a clearer understanding of the corrosion risk for such pipelines. Different CO_2 phases (liquid and supercritical), concentrations of SO_2 (< 1%) and flow velocities were used in an autoclave based study. The corrosion rate of steel samples was determined by weight loss measurements. The surface morphology and the composition of the corrosion product layers were analyzed by using surface analytical techniques (SEM, EDS, and IFM). Results showed that the corrosion rate decreased with decreasing SO_2 content in the supercritical CO_2 phase containing 650 ppm of water. In addition, significant localized corrosion was observed when CO_2 phase was liquid.

Keywords: CO_2 corrosion, CCS, liquid and supercritical CO_2, CO_2 transport, SO_2

INTRODUCTION

It has been acknowledged that green house gas (GHG) emissions due to human activities such as carbon dioxide (CO_2), methane (CH_4) and nitrous oxide N_2O, are one of the principal reasons for climate change. Among them, CO_2 has been given much attention because CO_2 emissions from fossil fuel combustion have been increasing at an average annual rate of 0.4 percent from 1990 to 2009, representing 79 percent of the total emissions in 2009.[1] Coal, natural gas and oil fired power plants are together the largest CO_2 emitter. One way to reduce CO_2 emissions to the atmosphere is through carbon capture and storage (CCS). This method consists of capturing CO_2 at the source, transporting it to suitable storage site, and sequestering it in geological formations such as oil and gas reservoirs, deep saline aquifers and coal beds.[2]

One of the ways for transporting CO_2 from the point sources to storage sites is through pipelines manufactured from high strength steel X65 and X70.[4] Due to high pressures, the CO_2 in these pipelines is typically in supercritical or liquid phase. Depending on the source and capture process, the CO_2 can contain impurities.[3] Before the CO_2 is injected in the pipeline it is sufficiently dried in order to avoid the presence of free water and therefore reduce the likelihood of corrosion of the carbon steel. In the absence of impurities and with water below its solubility limit, it appears that the high pressure CO_2 is not corrosive to the steel.[5,6] However, the presence of impurities such as SO_2 and O_2 increases the likelihood of corrosion even if there is no free water in the system. [5-7]

Recently, several researches have been conducted on corrosion of materials in liquid and supercritical CO_2 contaminated by water, O_2, and SO_2. Beck *et al.,*[8] developed an experimental system for carrying out *in-situ* measurements of conductivity and steel corrosion in supercritical CO_2 fluids. Water-saturated supercritical CO_2 had a conductivity near 7×10^{-3} S/m, with dry supercritical CO_2 having a conductivity two orders of magnitude lower. In addition, they found that the passive layer that apparently formed on the metal surface during system pressurization in gaseous CO_2 further degraded over time under supercritical conditions.

Zhang *et al.,*[9] claimed that water mist saturated with supercritical CO_2 was corrosive for C-steels, however not for 13Cr or Cr-Ni steels even up to 130°C. In addition, they showed that droplets of water mist, saturated with supercritical CO_2, caused localized attack when touching the carbon steel surface.

Xiang *et al.,*[4] conducted corrosion experiments of X70 steel and iron in water-saturated supercritical CO_2 mixed with SO_2. The corrosion rate of X70 steel increased as the SO_2 concentration increased, and the corrosion products were mainly hydrates of $FeSO_4$ and $FeSO_3$. They claimed that the presence of SO_2 intensifies the corrosiveness of the water saturated supercritical CO_2, and the corrosion caused by SO_2 is much more intense than that caused by CO_2.

Dugstad *et al.,*[6] showed that dense phase (liquid) CO_2 with water content significantly lower than the solubility limit is non corrosive. However, corrosion can take place in dense phase CO_2 at a water content of 200 ppm (wt) when SO_2 and O_2 are present.

Choi et al.,[10] studied the effect of water content on the corrosion of carbon steel in supercritical CO_2/O_2 phase. It was found that as long as the water content is kept below its solubility limit in CO_2 (3300 ppm at 80 bar and 50°C) no significant attack will take place. However, it was also reported that the addition of 1% SO_2 in the gas phase dramatically increased the corrosion rate

of carbon steel to 3.5 mm/y with only 650 ppm of water, concentration, which is significantly below the solubility limit in CO_2 and the current unofficial industry standard: the so called Kinder Morgan specification for transporting CO_2 in pipelines.[10]

Considering the real situations for CO_2 transport pipelines, effects of CO_2 phase and SO_2 concentration should be further qualified in order to establish a clear understanding of the corrosion risk for such pipelines. Therefore, the present study aimed at studying the corrosion behavior of carbon steel exposed to liquid and supercritical CO_2 with impurities such as water (below the solubility limit: 650 ppm) and SO_2 (small amounts: < 1%). In order to achieve these goals, corrosion tests were performed in an autoclave. Corrosion rate of samples were determined by weight loss measurements. The morphology and compositions of corrosion products were analyzed by scanning electron microscopy (SEM) and energy dispersive X-ray spectroscopy (EDS). In order to measure the pit depth when localized was observed an infinite focus microscope (IFM) was used. Some preliminary results about the effect of flow in liquid and supercritical CO_2 are also reported.

EXPERIMENTAL PROCEDURE

Corrosion tests were performed in a 1000 mL 316 stainless steel autoclave. A schematic drawing of the pressurized system is shown in Figure 1. Test samples were machined from API 5L[(1)] X65 pipeline steel with a 10.7 cm^2 exposed area. At one end of the samples, a 1 mm diameter hole was made in order to hang them inside the autoclave. Table 1 shows the chemical composition of the pipeline steel used for the corrosion tests.

Before each experiment the samples were ground with 600 grit silicon carbide paper, cleaned with isopropyl alcohol in an ultrasonic bath, dried and weighed using a balance with a precision of 0.1 mg. Two samples were placed inside the autoclave and 650 ppm (mole) of DI water was added at the bottom of the system. The amount of water was chosen taking into account the drying requirement for CO_2 pipelines used for enhanced oil recovery (EOR) in the United States which is 650 ppm (mole) maximum.[11] Once sealed, the autoclave temperature was adjusted. Then, a technical grade SO_2 was directly injected into the autoclave to the desired pressure. Finally, high pressure CO_2 was added to the autoclave with a gas booster pump to the desired working pressure. Details of the experimental matrix are given in Table 2.

Figure 2 shows the phase diagram for pure CO_2 and in the presence of different SO_2 amounts. Values for the critical points for pure CO_2 and CO_2/SO_2 mixtures are reported in Table 2.[12] At pressures and temperatures above the critical point the CO_2 is present in a supercritical state. At pressures above, and temperatures below the critical point, the CO_2 exists as a liquid. Usually, the presence of impurities causes the formation of a two phase gas-liquid region[13], however, as shown in Figure 2 and Table 3, the presence of SO_2 does not have a big influence neither on the formation of a two phase region nor on the critical points.

([1]) American Petroleum Institute (API), 1220 L St. NW, Washington, DC 20005.

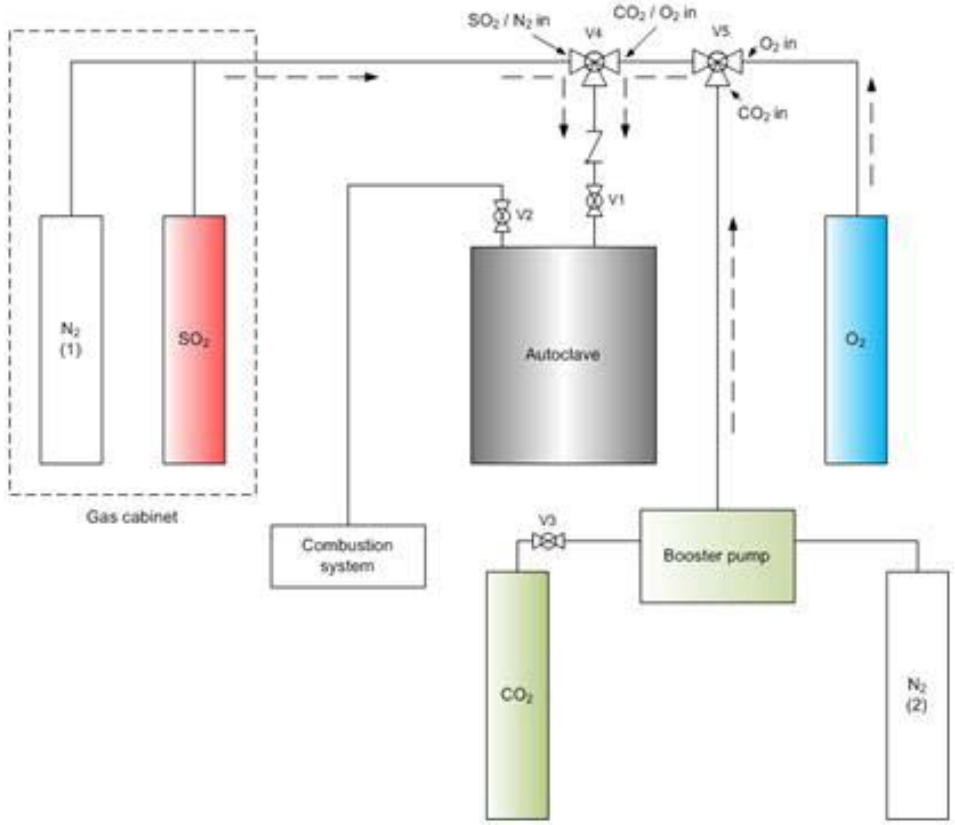

Figure 1: Schematic drawing of the CO_2/SO_2 pressurized system used for the corrosion tests.

TABLE 1

Elemental analysis for the carbon steel (API 5L X65) used in the corrosion tests (wt. %)

C	Mn	Si	P	S	Cr	Cu	Ni	Mo	Al	Fe
0.065	1.54	0.25	0.013	0.001	0.05	0.04	0.04	0.007	0.041	balance

TABLE 2

Experimental matrix for the corrosion tests

Parameter	Description
Material	API 5L X65
Solution	DI water (650 ppm)
Temperature (^oC)	25, 50
CO_2 partial pressure (bar)	80
SO_2 partial pressure (bar)	0.08, 0.04 (0.1 and 0.05% in gas phase)
CO_2 phase	Liquid, supercritical
Test methods	WL, SEM, EDS, IFM
Test period (hr)	24

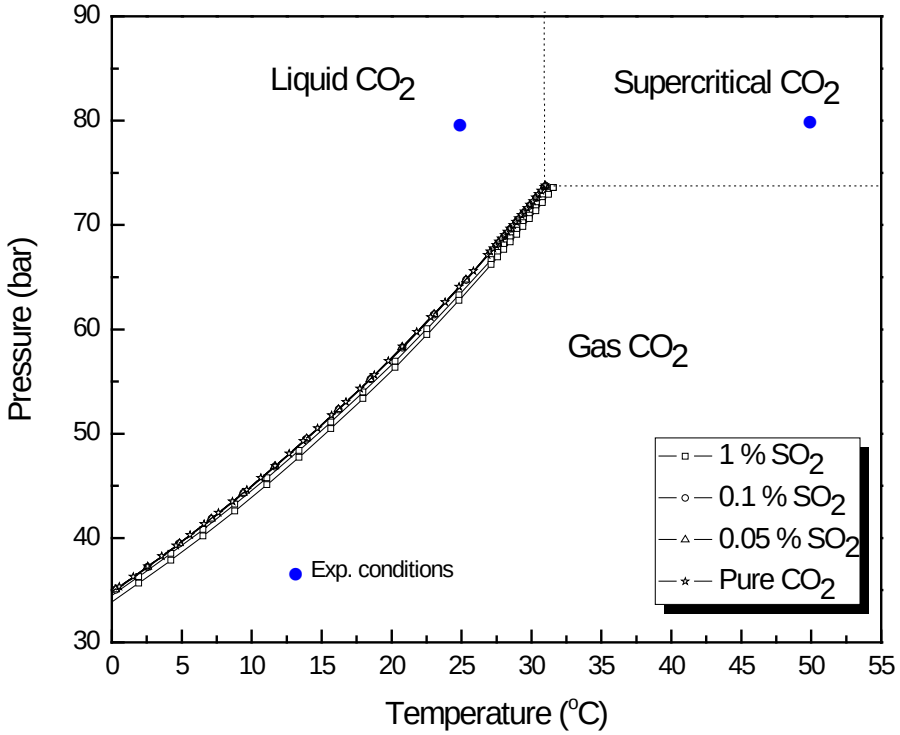

Figure 2: Phase diagram for CO_2 with different SO_2 amounts.[12]

TABLE 3

Critical point conditions for pure CO_2 and in the presence of SO_2.[12]

Component	Critical Pressure (bar)	Critical Temperature (^oC)
CO_2	73.77	30.97
CO_2 + 0.05% SO_2	73.76	31.00
CO_2 + 0.1% SO_2	73.75	31.03
CO_2 + 1.0% SO_2	73.57	31.55

The weight–loss method was used to calculate the average corrosion rate for two samples which were simultaneously exposed to the aggressive environment for 24 hours. After surface analysis, the samples were cleaned using the Clarke solution,[14] rinsed in DI water, dried and weighed. Equation 1 was used to calculate the average corrosion rate: [15]

$$CR = \frac{8.76 \times 10^4 (\text{mm} \cdot \text{hour/cm} \cdot \text{year}) \times \text{weight loss (g)}}{\text{area (cm}^2) \times \text{density (g/cm}^3) \times \text{time (hour)}} \quad (1)$$

The morphology and compositions of corrosion products were analyzed by scanning electron microscopy (SEM) and energy dispersive X-ray spectroscopy (EDS). In order to measure the pit depths when localized was observed, an infinite focus microscope (IFM) was used.

RESULTS

Corrosion tests in supercritical CO_2 with impurities

In the absence of SO_2 and when the water is kept below its solubility limit in supercritical CO_2, no corrosion has been observed.[5] However, the presence of SO_2 in the system can increase the corrosion rate. The effect of SO_2 concentration on the corrosion rate of an API 5L X65 steel exposed to supercritical CO_2/SO_2 phase is shown in Figure 3. Corrosion rate at 1% SO_2 (0.8 bar) was reported in a previous study and it is reproduced here as a reference point.[10] It can be observed that the corrosion rate decreased sharply when SO_2 concentration was reduced from 1% (0.8 bar) to 0.1% (0.08 bar). A further decrease in SO_2 content did not show any effect in the corrosion rate and no significant difference between 0.1% and 0.05% (0.04 bar) was observed.

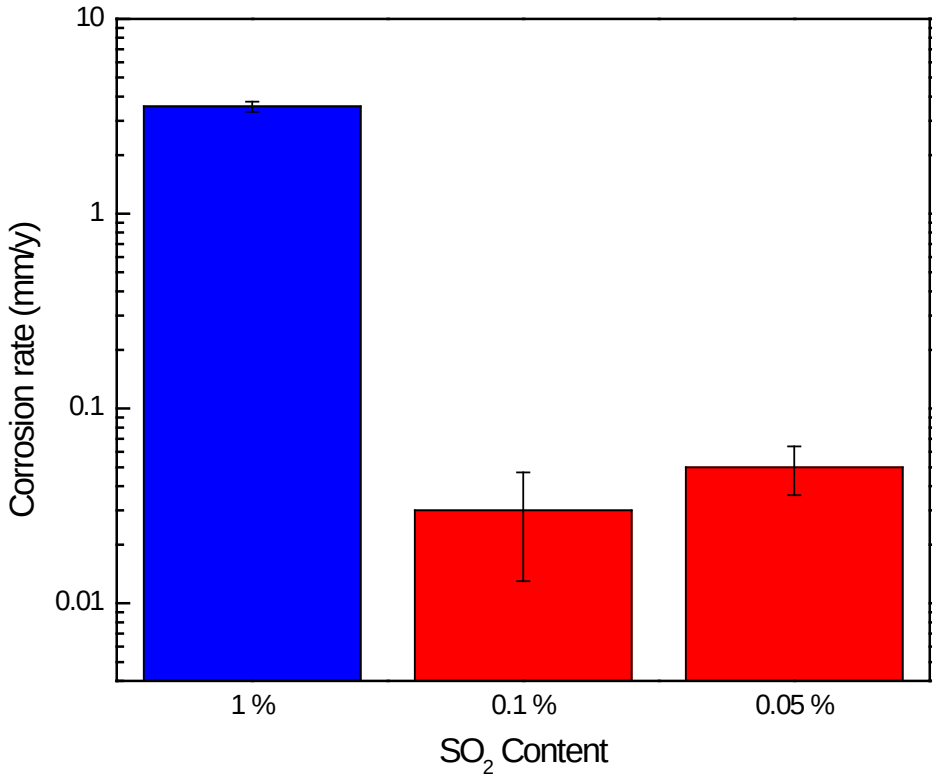

Figure 3: Effect of SO_2 concentration on the corrosion rate of carbon steel exposed in the supercritical CO_2 phase for 24 h, at a CO_2 partial pressure of 80 bar, 50°C, with 650 ppm water.

Figure 4 shows the surface morphology of the corroded WL coupons at different SO_2 concentrations exposed for 24 h in the supercritical CO_2/SO_2 phase with 650 ppm of water. Figure 4(a) was already reported in a previous publication[10] and it is shown here as a comparison point for the other experimental conditions. Figure 4(a) shows a surface covered by a dendritic corrosion product. According to Choi *et al*.,[10] the corrosion product was a mixture of hydrated $FeSO_3$ and $FeSO_4$. The formation of $FeSO_3$ and $FeSO_4$ in the presence of SO_2 and water can be explained by the following reactions:[10]

$$SO_2 + H_2O \rightarrow SO_3^{2-} + 2H^+ \quad (2)$$

$$Fe^{2+} + SO_3^{2-} \rightarrow FeSO_3 \quad (3)$$

$$SO_3^{2-} + H_2O \rightarrow SO_4^{2-} + 2H^+ + 2e^- \quad (4)$$

$$Fe^{2+} + SO_4^{2-} \rightarrow FeSO_4 \quad (5)$$

The surface of the samples for 0.1% and 0.05% SO_2 are shown in Figure 4(b) and 3(c), respectively. No visible signs of corrosion were observed for both conditions even at high magnification, i.e. the steel surfaces showed polishing marks and an absence of any corrosion products, what is in qualitative agreement with the low corrosion rate obtained by WL.

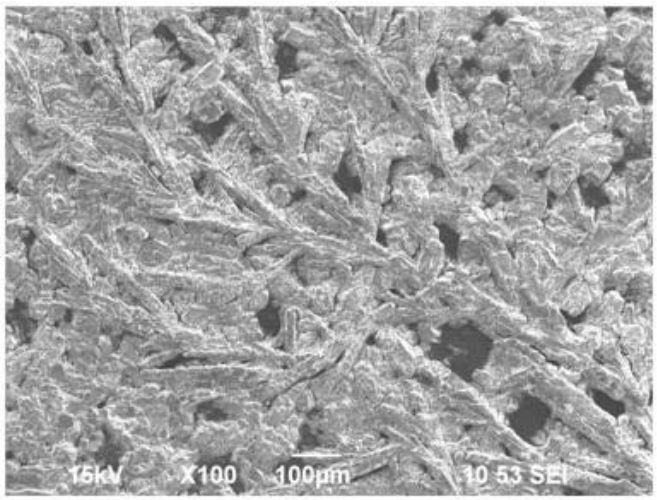

(a)

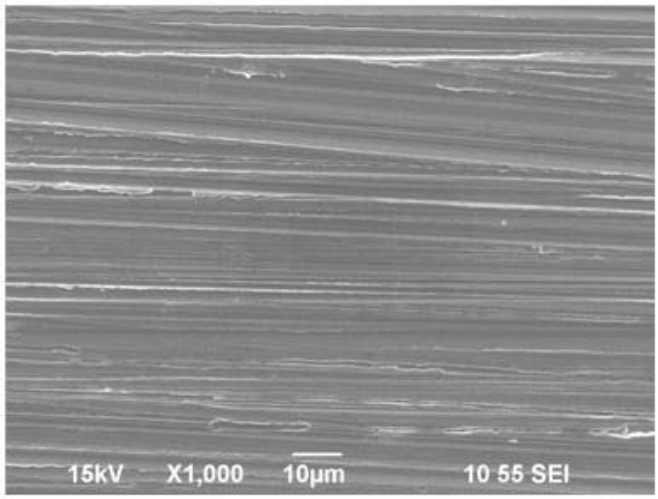

(b)

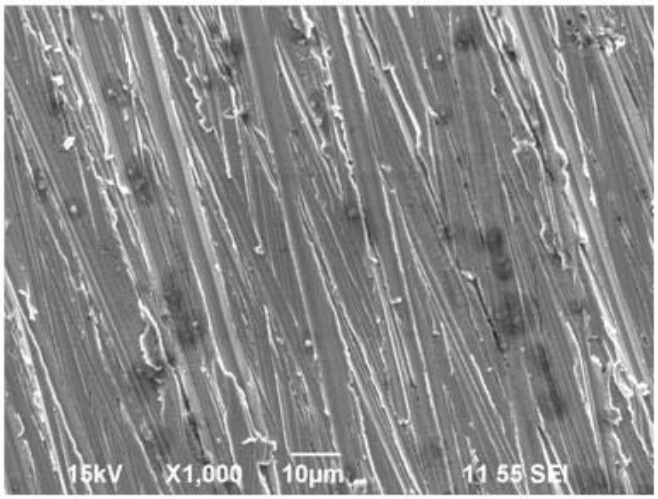

(c)

Figure 4: SEM pictures of WL coupons surface after being exposed for 24 h in supercritical CO_2 phase, at a CO_2 partial pressure of 80 bar, 50°C, with 650 ppm water: (a) 1.0% SO_2, (b) 0.1% SO_2, (c) 0.05% SO_2.

Corrosion tests in liquid CO_2 with impurities

Tests in supercritical CO_2/SO_2 phase described above revealed that corrosion of carbon steel can take place even if the concentration of water (650 ppm) is below its solubility limit. However, corrosion rate was negligible when SO_2 concentration was below 0.1%. On the other hand, during the transport of CO_2 in pipelines, CO_2 can be either in liquid or supercritical phase. Therefore, it is also important to study the behavior of carbon steels when exposed to liquid CO_2 with impurities such as water and SO_2.

Figure 6 shows the corrosion rates of carbon steel exposed to a liquid CO_2 phase (80bar CO_2, 25°C) with different SO_2 contents. Although the general corrosion rates were low in the liquid CO_2 phase with 0.1% SO_2 (≈ 0.1 mm/y), the corrosion rates measured in the liquid CO_2 phase showed higher values than were measured in the supercritical CO_2 phase (≈ 0.03 mm/y). However, in liquid CO_2 with only 0.05% SO_2, there was no measurable specimen weight change (less than 0.1 mg/cm^2) after 24 hours, indicating an insignificant corrosion rate.

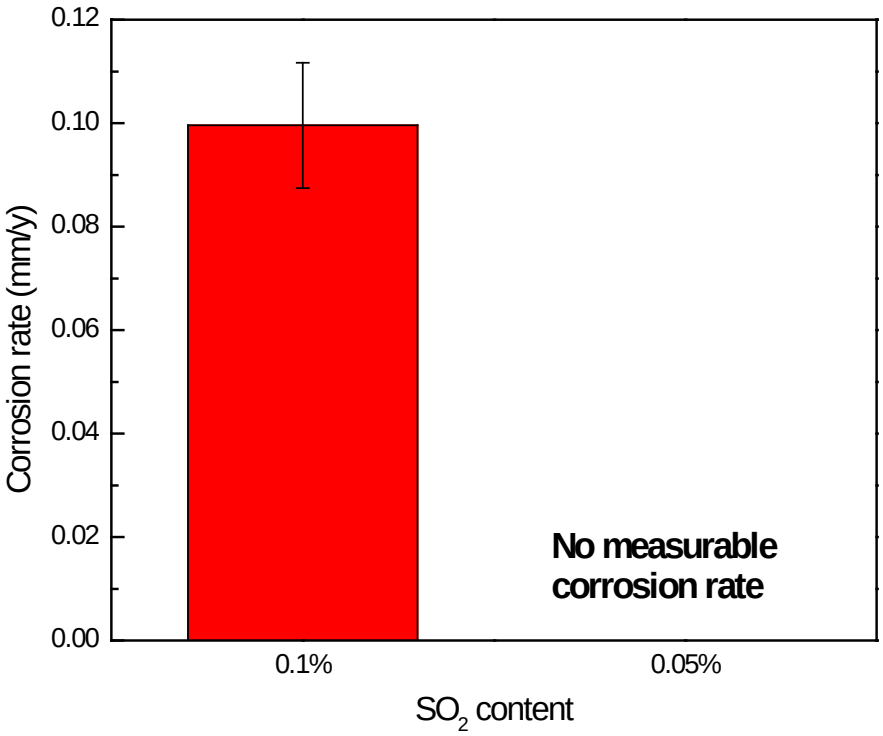

Figure 5: Effect of SO_2 content on the corrosion rate of carbon steel exposed in the liquid CO_2 phase for 24 h, at a CO_2 partial pressure of 80 bar, 50°C, with 650 ppm water.

Observation of the corrosion surface of the sample exposed to liquid CO_2/SO_2 phase with 0.1% SO_2 revealed the presence of heterogeneous, globular corrosion products in an otherwise uniformly cracked layer (Figure 6(a)). According to the chemical analysis performed by EDS (Figure 6(b)), the globular corrosion product consisted mainly of iron, oxygen and sulfur. The cracked layer indicated the same chemical elements by the EDS analysis (not

shown here). In previous research study, this corrosion product was reported to be hydrated $FeSO_3$ and $FeSO_4$.[10]

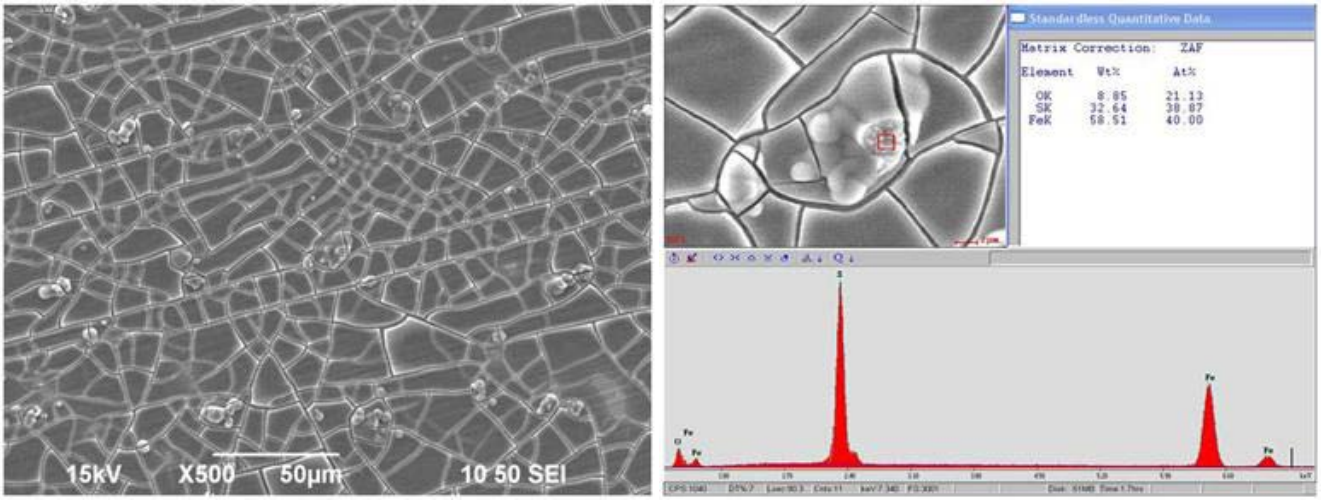

(a) (b)

Figure 6: SEM image (a) and EDS analysis (b) of the corroded surface of the coupon exposed to the liquid CO_2 for 24 h, at a CO_2 partial pressure of 80 bar, 50°C, with 0.1% SO_2.

Figure 7(a) shows the corroded surface of the metal sample after being exposed to a liquid CO_2 phase with 0.05% SO_2. Although no significant corrosion rate was measured, a globular corrosion product was found on the metal surface. EDS analysis (Figure 7(a)) revealed the presence iron, oxygen and sulfur. Comparing Figure 7(b) with Figure 6(b) observed a less intense sulfur peak is observed that can be ascribed to the decrease in SO_2 content.

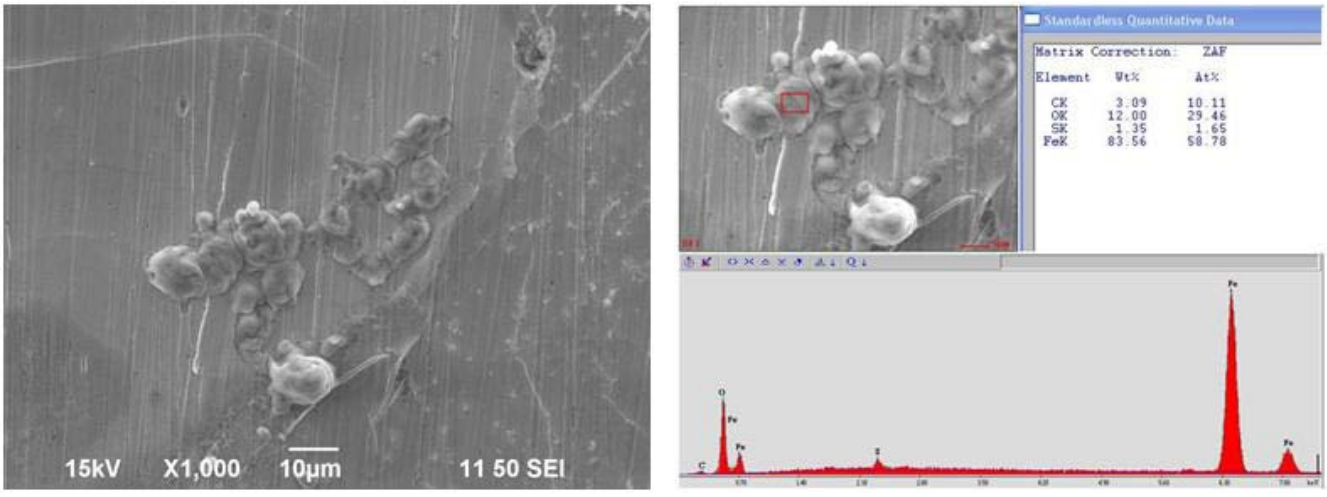

(a) (b)

Figure 7: SEM image and EDS spectra of the corroded surface of the sample exposed to the liquid CO_2 for 24 h, at a CO_2 partial pressure of 80 bar, 50°C, with 0.05% SO_2.

Figure 8 shows the surface morphologies of the two samples after cleaning with Clarke solution. Localized attack was observed for both conditions, being more severe with 0.1% SO_2 than 0.05% SO_2. This suggests that localized corrosion could be accelerated by increasing SO_2 concentration. Furthermore, it implies that even though uniform corrosion rate from the weight loss measurement was low, localized corrosion can be initiated in the liquid CO_2 phase with SO_2.

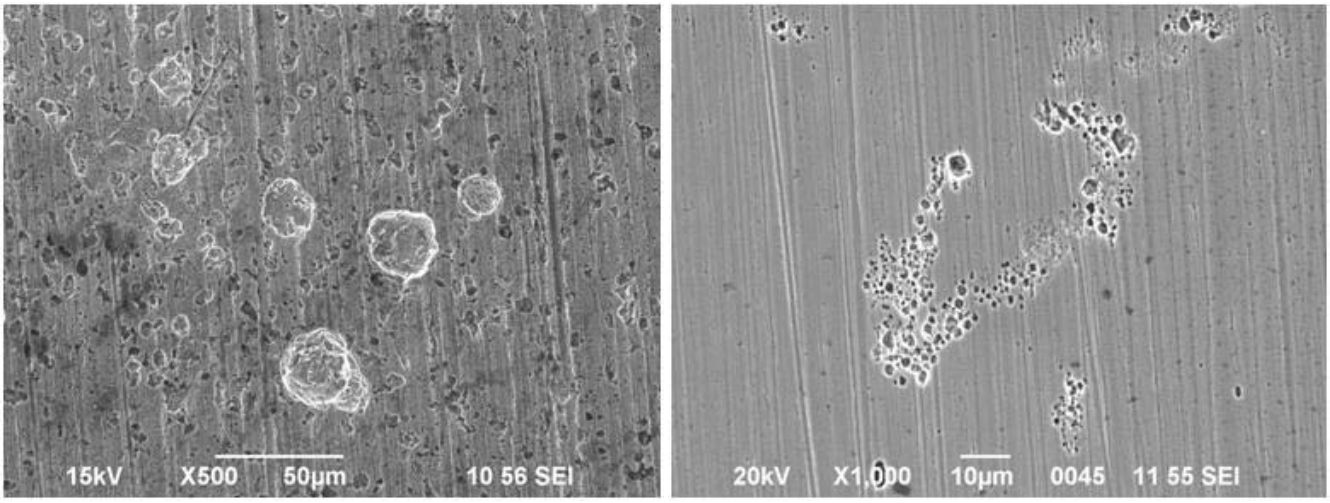

Figure 8: SEM images of the corroded surface of the samples exposed to the liquid CO_2 for 24 h, at a CO_2 partial pressure of 80 bar, 50°C, after cleaning: (a) 0.1% SO_2, (b) 0.05% SO_2.

Figure 9 and Figure 10 present the results of Infinite Focus Microscope (IFM) analysis of several pits observed on the cleaned sample exposed to the liquid CO_2 for 24 h, at a CO_2 partial pressure of 80 bar, 50°C. According to the depth of the deepest pit measured by IFM, the maximum localized corrosion rates were calculated for each condition and shown in Table 3.

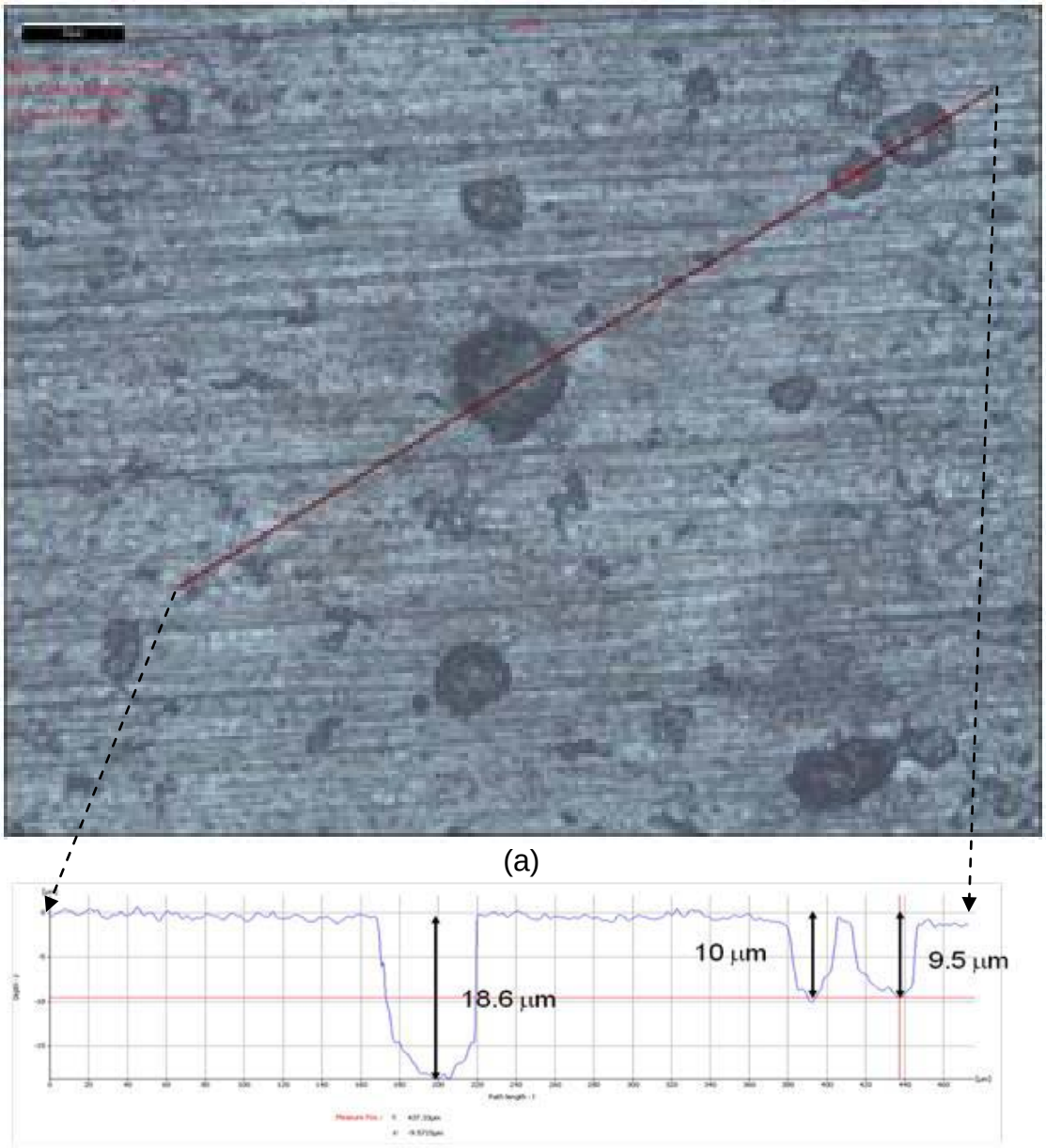

Figure 9: IFM analysis of the pits on the sample exposed to liquid CO_2 with 0.1% SO_2 for 24 h, at a CO_2 partial pressure of 80 bar, 50°C, after cleaning: (a) optical image of the pits, (b) measured depth of the pits.

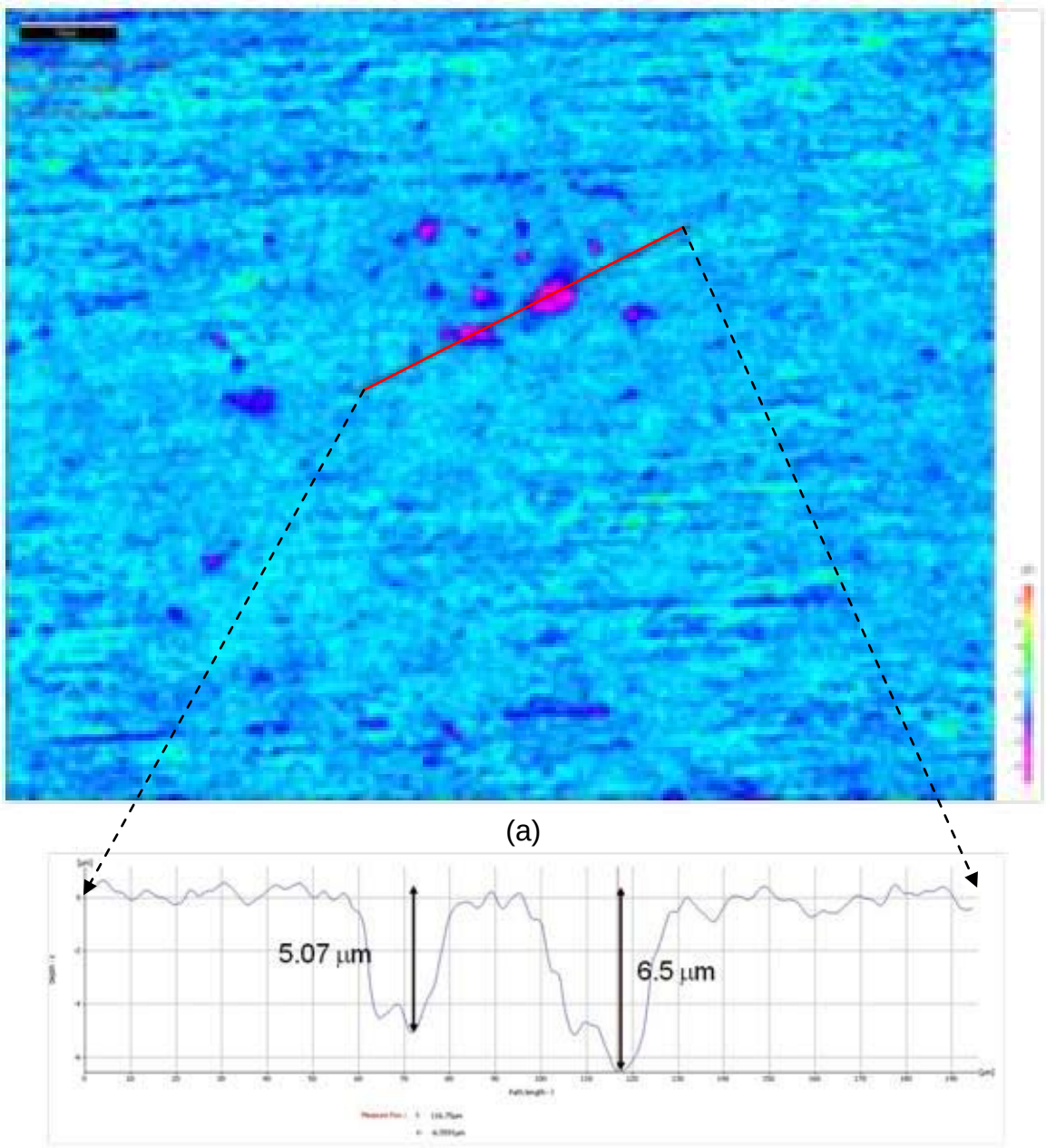

Figure 10: IFM analysis of the pits on the sample exposed to liquid CO_2 with 0.05% SO_2 for 24 h, at a CO_2 partial pressure of 80 bar, 50°C, after cleaning: (a) optical image of the pits, (b) measured depth of the pits.

TABLE 3

Comparison of corrosion rates obtained from weight loss measurements and IFM analysis of pit penetration depth for samples exposed to liquid CO_2 for 24 h, at a CO_2 partial pressure of 80 bar, 50°C, after cleaning at different SO_2 contents in the liquid CO_2 phase.

	Corrosion rate from weight loss (mm/y)	Maximum pit depth from IFM (μm)	Localized corrosion rate (mm/y)
0.1% SO_2	0.1	18.6	6.8
0.05% SO_2	≈ 0	6.5	2.4

Effect of flow on the corrosion of carbon steel in liquid and supercritical $CO_2/H_2O/SO_2$ environments

In order to investigate the effect of flow on the corrosion behavior of carbon steel, stirred autoclave corrosion experiments were conducted in both supercritical and liquid CO_2 phases with SO_2. Intense stirring (i.e. 1000 rpm) was achieved using a stainless steel impeller at the bottom of the autoclave.

Figure 11 shows some preliminary results in flowing conditions for the corrosion rates of carbon steel in the supercritical CO_2 (80 bar CO_2, 0.08 bar SO_2, 50°C) and liquid CO_2 (80bar CO_2, 0.08 bar SO_2, 25°C) with 650 ppm water. It is interesting to note that the corrosion rates for both conditions showed lower values than those without flow. Especially, the corrosion rate in the liquid CO_2 phase decreased from 0.1 mm/y (without flow) to 0.013 mm/y (with flow).

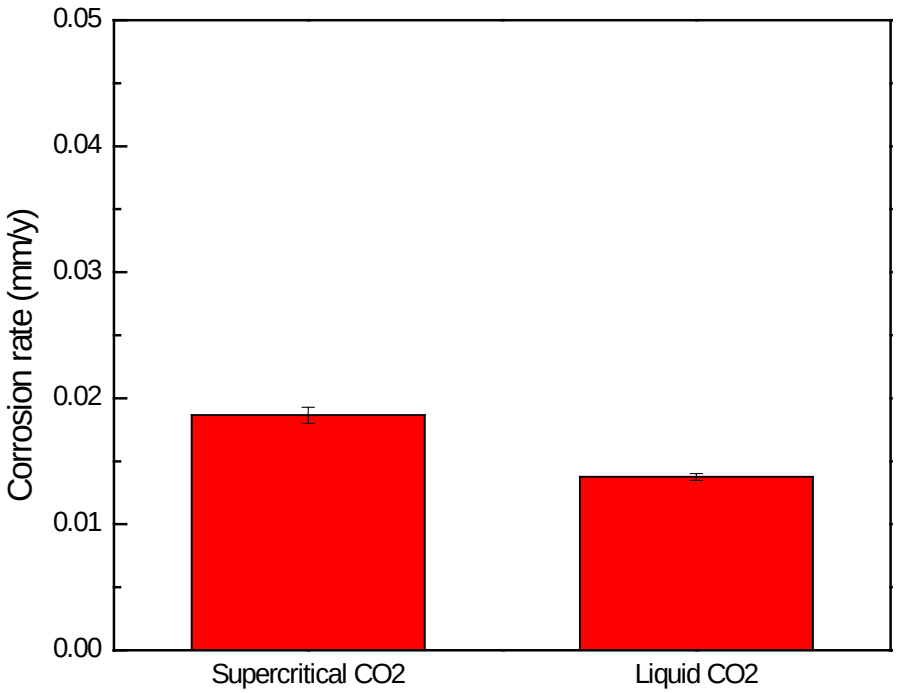

Figure 11: Corrosion rates of carbon steel in supercritical and liquid CO_2 phases with flow, at 80 bar CO_2, 0.08 bar SO_2, 50°C and 650 ppm of water.

Figure 12 shows the SEM surface images of the samples exposed to the supercritical CO_2/SO_2 and liquid CO_2/SO_2 phases with flow. It can be seen that some corrosion product deposits formed on the steel surfaces for both conditions.

Figure 13 shows the surface morphology of the samples after cleaning with Clarke solution. No significant corrosion attack was observed on the sample for the supercritical CO_2 condition, *i.e.*, the surfaces showed clear polishing marks and are devoid of localized corrosion. However, some pits were observed on the surface for the liquid CO_2 condition, suggesting localized corrosion risk, even if these pits were very small and shallow. Further research is ongoing in order to understand the effect of flow on the corrosion of steel in liquid and supercritical $CO_2/H_2O/SO_2$ environments**.**

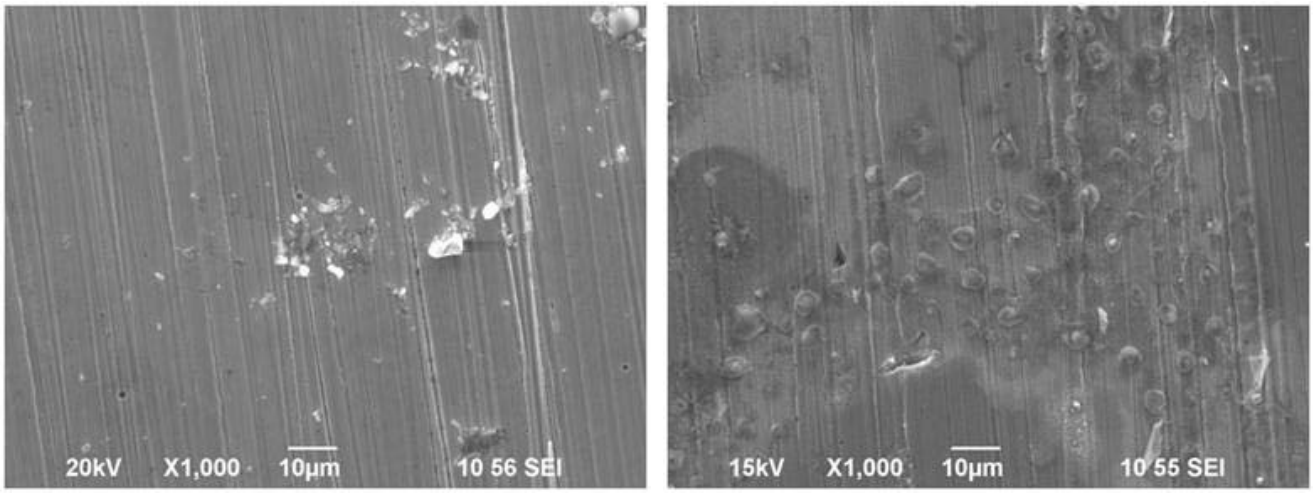

(a) (b)

Figure 12: SEM images of the corroded surface of the samples exposed to a flowing CO_2 at 80 bar CO_2, 0.08 bar SO_2, and 650 ppm of water: (a) supercritical CO_2 and (b) liquid CO_2 .

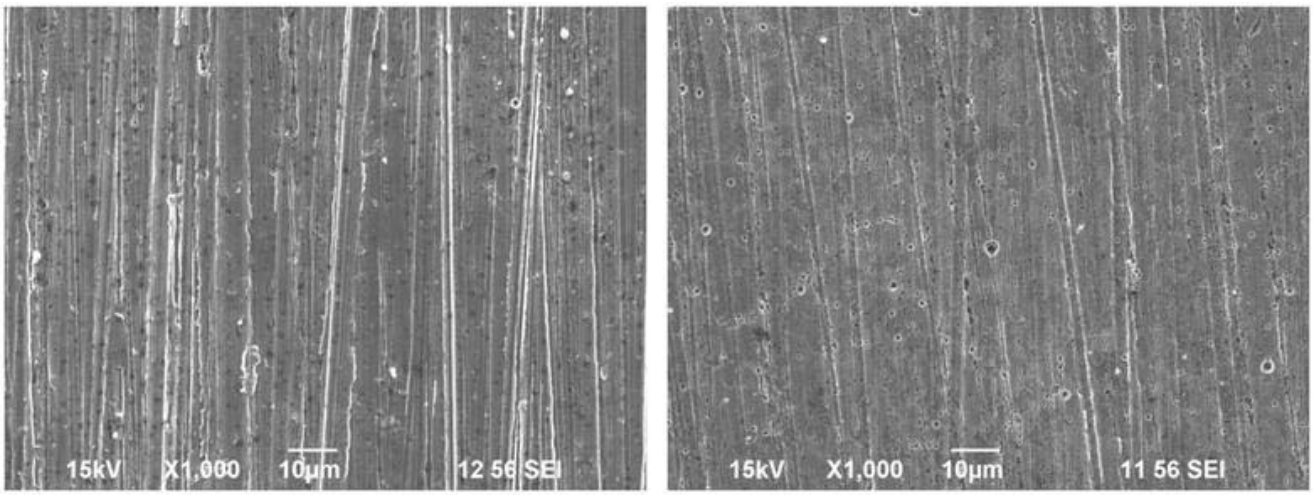

(a) (b)

Figure 13: SEM images of the cleaned corroded surface of the samples exposed to a flowing CO_2 at 80 bar CO_2, 0.08 bar SO_2, and 650 ppm of water: (a) supercritical CO_2 and (b) liquid CO_2 .

CONCLUSIONS

- In the high pressure supercritical CO_2 systems containing 650 ppm water, the concentration of SO_2 less than 0.1% did not lead to significant corrosion of carbon steel, in short term experiments.
- In high pressure liquid CO_2 conditions with 650 ppm of water and 0.05% SO_2, localized attack was seen with a rate about 2.4 mm/y, in short term experiments.

ACKNOWLEDGEMENTS

The authors would like to thank the financial support from Ohio Coal Development Office (OCDO) given to the Institute for Corrosion and Multiphase Technology at Ohio University.

REFERENCES

1. U.S. Environmental Protection Agency Report, Inventory of U.S. Greenhouse Gas Emissions and Sinks: 1990 – 2009, (2011), p.7.

2. Metz BO, Davidson H, de Coninck C, Loos M, Meyer LA editors. IPCC Special Report on Carbon Dioxide Capture and Storage. Prepared by working group III of the intergovernmental panel on climate change. Cambridge, United Kingdom and New York, NY, USA: Cambridge University Press; 2005.

3. E. de Visser, C. Hendriks, M. Barrio, M.J. Molnvik, G. de Koeijer, S. Liljemark, Y. Le Gallo, Dynamis CO_2 Quality Recommendations, International Journal of Greenhouse Gas Control 2 (2008) 478 - 484.

4. Y. Xiang, Z. Wang, C. Xu, C. Zhou, Z. Li, W. Ni, Impact of SO_2 Concentration on the Corrosion Rate of X70 Steel and Iron in Water-saturated Supercritical CO_2 mixed with SO_2, J. of Supercritical Fluids 58 (2011) 286-294.

5. Y.S. Choi and S. Nesic, Effect of Water Content on the Corrosion Behavior of Carbon Steel in Supercritical CO_2 Phase with Impurities, CORROSION/2011, paper no. 11377 (Houston, TX: NACE, 2011).

6. A. Dugstad, S. Clausen, B. Morland, Transport of Dense Phase CO_2 in C-steel Pipelines – When is Corrosion an Issue?, CORROSION/2011, paper no. 11070 (Houston, TX: NACE, 2011).

7. F. Ayello, K. Evans, R. Thodla, and N. Sridhar, Effect of Impurities on Corrosion of Steel in Supercritical CO_2, CORROSION/2010, paper no. 10193 (Houston, TX: NACE, 2010).

8. J. Beck, S. Lvov, M. Fedkin, M. Ziomek-Moroz, G. Holcomb, J. Tylczak, D. Alman, Electrochemical System to Study Corrosion of Metals in Supercritical CO_2 Fluids, CORROSION/2011, paper no. 11380 (Houston, TX: NACE, 2011).

9. Y. Zhang, K. Gao, and G. Schmitt, Water Effect on Steel under Supercritical CO_2 Conditions, CORROSION/2011, paper no. 11378 (Houston, TX: NACE, 2011).

10. Y.S. Choi, and S. Nesic, Effect of Water Content on the Corrosion Behavior of Carbon Steel in Supercritical CO2 phase with impurities, CORROSION/2011, paper no. 11377 (Houston, TX: NACE, 2011).

11. D.P. Connell, Carbon Dioxide Capture Options for Large Point Sources in the Midwestern United States: An Assessment of Candidate Technologies, Final Report, CONSOL Energy Inc., p. 7 (2005).

12. E.W. Lemmon, M.L. Huber, M.O. McLinden, NIST Standard Reference Database 23: Reference Fluid Thermodynamic and Transport Properties-REFPROP, Version 9.0, National Institute of Standards and Technology, Standard Reference Data Program, Gaithersburg, 2010.

13. P. N. Seevam, P. Hopkins, Trasporting the Next Generation of CO_2 for Carbon, Capture and Storage: The Impact of Impurities on Supercritical CO_2 Pipelines, Proceedings of IPC2008, 7th International Pipeline Conference, September 29-October 3, 2008, Carlgary, Alberta, Canada.

14. ASTM Standard G1-03, Standard Practice for Preparing, Cleaning and Evaluating Corrosion Test Specimens, Annual Book of ASTM Standards, vol. 03. 02 (West Conshohocken, PA: ASTM International, 2003).

15. ASTM Standard G1-03, Standard Practice for Preparing, Cleaning and Evaluating Corrosion Test Specimens, Annual Book of ASTM Standards, vol. 03. 02 (West Conshohocken, PA: ASTM International, 2003).